*Sensors and Materials*, Vol. 37, No. 4 (2025) 1351–1362
MYU Tokyo


S & M 3991

# Suppression of Drift in Ion-selective Field Effect Transistor by UV Light Irradiation

Yasumichi Takase,[1*] Takafumi Ishigaki,[1] Shinnosuke Nakamura,[1]
Hideaki Asao,[1] Tomoko Horio,[2] Takeshi Hizawa,[2]
Yasuyuki Kimura,[2] Kazuaki Sawada,[2] and Atsuomi Fukuura[1]

[1]Keihanna R&D Center, Kyocera Corporation, 3-5-3 Hikaridai, Seika-cho, Kyoto 619-0237, Japan
[2]Department of Electrical and Electronic Information Engineering, Toyohashi University of Technology,
1-1 Hibarigaoka, Tempaku-cho, Toyohashi, Aichi 441-8122, Japan

(Received February 3, 2025; accepted March 17, 2025)

***Keywords:*** ion-selective field-effect transistor, drift, light irradiation, charge trapping, interface trap

Ion-selective field-effect transistors (ISFETs) are a type of potentiometric sensor with a wide range of potential applications. However, the application of ISFETs is hindered by the instability of the threshold voltage ($V_T$), known as the drift. In this study, we hypothesized that the charge trapping at the interface between the oxide layer and the Si substrate of ISFETs affects the drift, and we examined the effects of the irradiation of UV light on the drift. To investigate the drift more simply, we fabricated a Si wafer sample with a 30 nm $Al_2O_3$ layer, which is regarded as the sensing layer of an ISFET, and we measured the drift by capacitance–voltage measurements using an electrochemical cell. Results showed that the amount of drift after light irradiation decreased to 6.6% (37 mV/h) relative to the original drift (558 mV/h) in the best case. It was also suggested that the drift is caused by multiple charge trapping mechanisms. These results indicate that charge trapping is a cause of drift, and light irradiation can be used to suppress drift.

## 1. Introduction

Ion-selective field-effect transistors (ISFETs) are a type of potentiometric sensor that replaced the gate electrode of a metal-oxide-semiconductor field-effect transistor (MOSFET) with a sensing layer, an electrolyte, and a reference electrode.(1,2) The concept of ISFETs was originally proposed by Bergveld in the early 1970s.(3) Since the ISFETs have many advantages such as their amenability to miniaturization, quick response, compatibility with integrated circuits, and low output impedance, they have been intensively studied for various applications: the detection of biomolecules,(4) the measurement of ion concentrations in the soil and water,(5) the monitoring of cell activities,(6) the observation of the Belousov–Zhabotinsky reaction,(7) the fabrication of wearable ion-sensing devices,(8) the observation of the activities of neural cells in the brain,(9) and non-optical DNA sequencing.(10)

*Corresponding author: e-mail: yasumichi.takase@gmail.com
https://doi.org/10.18494/SAM5590

ISSN 0914-4935 
https://myukk.org/

However, the application of ISFETs is hindered by the problem of threshold voltage ($V_T$) instability, known as the drift.[11–14] To explain the mechanism of the drift, several models have been proposed focusing on the interface between the sensing layer and the electrolyte. These models explain the cause of the drift from the viewpoints of the hydration of the surface of the sensing layer,[15] the adsorption of molecules,[16] and oxide etching.[17] On the other hand, in the case of MOSFETs, it has been reported that the interface between the sensing layer and the Si substrate causes the instability of $V_T$ since the interface traps and trap levels in the oxide layer near the interface (border traps) trap charges in the Si substrate.[18]

The studies of MOSFETs, which have $Al_2O_3$ as the oxide layer, indicated that the application of a positive bias voltage induces the trapping of electrons, resulting in the positive change of $V_T$.[19–23] It was also reported that charge trapping and detrapping are promoted by light irradiation during the application of the bias voltage.[24–28] These results suggest that the drift caused by charge trapping may not be negligible also in ISFETs and the drift may be affected by light irradiation as in the case of MOSFETs.

In this research, we examined the effects of light irradiation on the drift in an ISFET. We focused on the drift in an ISFET with the $Al_2O_3$ sensing layer directly deposited on a p-type Si substrate, and we fabricated a wafer sample with the same layer composition. We measured the drift of the wafer sample by capacitance–voltage (CV) measurements[29] and examined the effects of UV light irradiation on the drift.

## 2. Data, Materials, and Methods

In this research, we used a p-type Si (100) wafer with a thickness of 525 µm and a resistivity of 1–10 Ω·cm. To remove the native oxide layer, the wafer was rinsed in 1% HF solution for 1 min followed by deionized water, and the sample was dried by blowing nitrogen. On the Si substrate, a layer of $Al_2O_3$ with a thickness of 30 nm was formed by atomic layer deposition (ALD) at 200 ℃ using trimethylaluminum (TMA) as the precursor of Al and $O_3$ as the oxidant. ALD was performed using internally manufactured ALD equipment, and the thickness of the $Al_2O_3$ layer was confirmed by X-ray reflectometry. On the opposite side of the Si wafer, a 10-nm-thick Cr layer and a 100-nm-thick Al layer were deposited by physical vapor deposition using EBX-2000 (ULVAK, Inc., Japan) to form the working electrode.

Figure 1 shows the setup of the CV measurements. All experiments were performed in an electromagnetic shield covered by a black curtain. The samples used in the CV measurements were prepared by cutting the wafer into square pieces of approximately 1 × 1 $cm^2$. For the CV measurements, a sample was placed on a Ni plate (The Nilaco Corp., Japan) with the working electrode side down, and the plate and the sample were then fixed to an electrochemical cell (VM2: EC Frontier Co., Ltd., Japan). The surface area of the sample was defined by a custom-made O-ring with an inner diameter of 6 mm; hence, the area was approximately 0.283 $cm^2$. An Ag/AgCl reference electrode (RE-T8A), a Pt counter electrode (CE-100: EC Frontier Co., Ltd., Japan), and a LED light with a peak wavelength of 395 nm (OptoSupply Ltd., China) powered by R6244 (Advantest Corp., Japan) were attached to the cap. The intensity of the light at the sample surface was measured by an optical power meter (8250A) and an optical sensor (82311: ADC

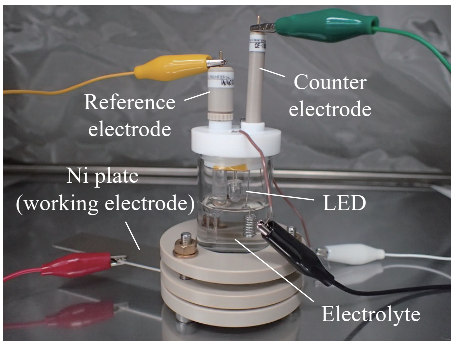


Fig. 1. (Color) Experimental setup of CV measurement and UV light irradiation.

Corp., Japan). The measurement wavelength of the power meter was set to 395 nm and the sensing part of the optical sensor was fixed to the cell. After putting on the cap, the intensity of the light without the electrolyte was adjusted to 1 mW. For the drift measurements, 14 mL of pH 6.86 phosphate buffer solution (FUJIFILM Wako Pure Chemical Corp., Japan) was used as the electrolyte.

CV measurements were started immediately after filling the cell with the electrolyte and covering the cell with the black curtain. The CV measurements were performed by using a frequency response analyzer (SI1260) and a potentiostat (SI1287: Solartron Analytical, UK). The frequency, the AC amplitude, and the sweep rate of the applied voltage were 1 kHz, 30 mV, and 50 mV/s, respectively. The sweep range of the voltage was from $V_{FB} - 3$ to $V_{FB} + 3$ V, where $V_{FB}$ is the flatband voltage of the wafer sample. $V_{FB}$ was determined by calculating the voltage at the flat band capacitance ($C_{FB}$), which is defined by the following equations:[29]

$$C_{FB} = \frac{C_{OX} C_{FBS}}{C_{OX} + C_{FBS}}, \tag{1}$$

$$C_{FBS} = \frac{\varepsilon_0 \varepsilon_{Si}}{\lambda}, \tag{2}$$

$$\lambda = \sqrt{\frac{\varepsilon_0 \varepsilon_{Si} k_B T}{q^2 N_A}}, \tag{3}$$

where $C_{OX}$ is the capacitance of the oxide layer per unit area, $C_{FBS}$ is the silicon surface capacitance at the flat band voltage per unit area, $\varepsilon_0$ is the vacuum permittivity, $\varepsilon_{Si}$ is the dielectric constant of Si, $\lambda$ is the Debye length, $k_B$ is the Boltzmann constant, $T$ is the temperature, $q$ is the elementary charge, and $N_A$ is the acceptor density per unit area. In the drift measurements, the DC bias voltage was applied for 5 min after the CV measurements, and the CV measurements and bias voltage application were repeated until the total time of the bias voltage application reached 60 min. The voltage applied to the reference electrode was $V_T + 1.1$ V, which is the bias voltage applied in an ISFET.[30] $V_T$ and $V_{FB}$ are given by Eqs. (4) and (5), respectively as follows:[31]

$$V_T = V_{FB} + 2\phi_B - \frac{Q_B}{C_{OX}}, \tag{4}$$

$$V_{FB} = E_{ref} - \psi_0 + \chi_{sol} - \frac{\Phi_{Si}}{q} - \frac{Q_{ss} + Q_{OX}}{C_{OX}}, \tag{5}$$

where $\varphi_B$ is the difference between the Fermi level and the intrinsic Fermi level, $Q_B$ is the depletion charge, $E_{ref}$ is the reference electrode potential relative to vacuum, $\psi_0$ is the surface potential caused by chemical reactions on the oxide surface, $\chi_{sol}$ is the surface dipole potential of the electrolyte, $\Phi_{Si}$ is the work function of Si, $Q_{ss}$ is the surface state density at the silicon surface, and $Q_{OX}$ is the fixed oxide charge. Since the pH of the electrolyte does not change during the measurements, these parameters are constant except for $Q_{ss}$ and $Q_{OX}$. $\varphi_B$ and $Q_B$ are calculated using Eqs. (6) and (7), respectively, as follows:[29]

$$Q_B = \sqrt{4\varepsilon_0 \varepsilon_{Si} q N_A \phi_B}, \tag{6}$$

$$\phi_B = \frac{k_B T}{q} \ln\left(\frac{N_A}{n_i}\right), \tag{7}$$

where $n_i$ is the intrinsic carrier concentration. In this research, $T$ and $\varepsilon_{Si}$ were 278 K and 11.7, respectively, and $N_A$ was $1 \times 10^{-16}$ cm$^{-3}$ on average. The $V_{FB}$ and $V_T$ of the sample were calculated by analyzing the results of CV measurements with the sweep range from –6.0 to 3.0 V, and determined as 1.791 and 2.864 V, respectively. Therefore, the initial sweep range of the CV measurements was set to –1.209 to 4.791 V by referring to the value of $V_{FB}$. The sweep range and the bias voltage were kept constant in the drift measurements. Every drift measurement was performed without light irradiation (dark condition), and the drift was quantified by the difference in $V_T$ from the initial value. To investigate the effect of light irradiation on $V_T$, UV light was irradiated during the application of the bias voltage, and the difference in $V_T$ caused by light irradiation ($\Delta V_T$) was calculated. The drifts after light irradiation were also analyzed to examine the effect of light irradiation on the drift.

## 3. Results

### 3.1 Measurement of drift without light irradiation

To estimate the drift without light irradiation, we first performed drift measurements under dark conditions. The bias voltage applied between CV measurements was $V_T$ + 1.1 V (3.964 V), and the CV measurements were repeated until the total time of the bias voltage application reached 60 min. The results of the CV measurements are shown in Fig. 2(a). As indicated by the black arrow, a shoulder is observed in the CV curves, which is interpreted as representing the amount of $Q_{ss}$.[29] Figure 2(a) also shows that the CV curves shift toward the direction of the

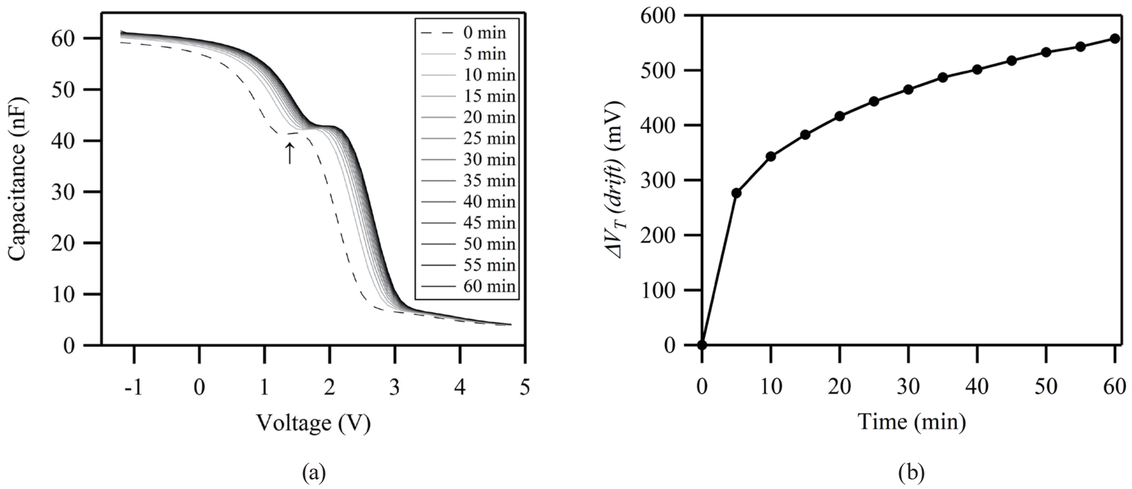


Fig. 2. Results of drift measurements under dark conditions. (a) Results of CV measurements. (b) $\Delta V_T$ caused by drift.

positive voltage over time and that the shift during 0–5 min is larger than the subsequent shifts. Figure 2(b) shows the drift of the sample. It shows that $\Delta V_T$ during 0–5 min (276 mV) is comparable to that during 5–60 min (281 mV) despite the difference in the duration of light irradiation, indicating that the mechanisms of drifts are different. Therefore, we divided the drift into two parts: the short-term (0–5 min) and long-term (5–60 min) drifts.

### 3.2 Effects of light irradiation on $V_T$

To examine the effect of light irradiation on $\Delta V_T$, light irradiation and CV measurements were performed repeatedly using the same sample. The duration of each light irradiation was 5 min and the bias voltage during light irradiation was $V_T$ + 1.1 V. CV measurements were performed before and after each light irradiation process to measure $\Delta V_T$ induced by light irradiation. The sweep range and bias voltage were updated from $V_{FB}$ – 3 V to $V_{FB}$ + 3 V and $V_T$ + 1.1 V, respectively, by using $V_T$ and $V_{FB}$ immediately after light irradiation. The CV measurements and light irradiation were repeated until the total time of light irradiation reached 50 min.

The results are shown in Fig. 3(a). The dashed and solid lines are the results of the CV measurements before and after light irradiation, respectively. The results obtained after the same total light irradiation duration are shown in the same color. Figure 3(a) shows that light irradiation induces significant shifts of the CV curves toward the positive voltage direction. It also shows that the shoulder in the CV curves disappears as the duration of light irradiation increases, which was not observed in the case of CV measurements under dark conditions [Fig. 2(a)]. The disappearance of the shoulder suggests that electrons were trapped by the trap levels in the oxide layer and the density of the trap levels had changed. Figure 3(b) shows $\Delta V_T$ (circle) and the bias voltage relative to the initial $V_T$ (triangle). It shows that both $\Delta V_T$ and bias voltage relative to the initial $V_T$ increase significantly. $\Delta V_T$ after the first light irradiation for 5 min is 965 mV,

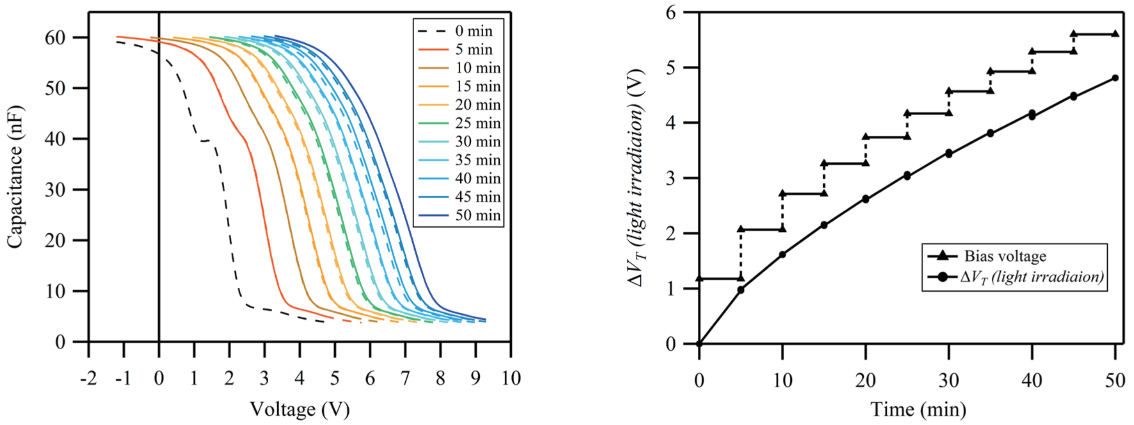


(a) (b)

Fig. 3. (Color) Effects of UV light irradiation on $V_T$. (a) Results of CV measurements before and after light irradiation (dashed and solid lines, respectively). (b) $\Delta V_T$ induced by UV light irradiation.

which is greater than the drift in 60 min under dark conditions [558 mV, Fig. 2(b)]. These results suggest that light irradiation promotes the trapping of electrons and induces a large positive change in $V_T$.

### 3.3 Effects of bias voltage in light irradiation on drift

Since light irradiation had significant effects on $V_T$, we also examined the drifts after light irradiation. We performed light irradiation for 5 min before the drift measurements and analyzed the light-irradiation-induced $\Delta V_T$ and the drift measurement results. The sweep range and bias voltage of the drift measurements were updated using the results of CV measurements after light irradiation with the sweep range from $V_{FB} - 3$ V to $V_{FB} + 7$ V. Regarding $\Delta V_T$ after light irradiation for 50 min [5.599 V, Fig. 3(b)], the bias voltage during light irradiation was varied at $V_T$ (2.864 V) + 2.1, 4.1, and 6.1 V. The drifts after the application of the bias voltage under dark conditions were also measured for comparison.

Figure 4(a) shows $\Delta V_T$ induced by light irradiation. It shows that $\Delta V_T$ after light irradiation is larger than those measured after bias voltage application under dark conditions. The drifts after bias voltage application with or without light irradiation are shown in Fig. 4(b). The figure shows that the total drifts after light irradiation were smaller than those measured after bias voltage application without light irradiation. Figure 4(c) presents the short-term (black) and long-term (gray) drifts of each sample. It shows that light irradiation is effective for suppressing the long-term drift, and the long-term drift is the smallest after the application of the bias voltage at $V_T$ + 6.1 V. It also shows that the short-term drift is suppressed by bias voltage application and that the short-term drift is not necessarily suppressed by light irradiation. The amount of short-term drift increases with the applied bias voltage before the drift measurement. These results suggest that there may be an optimal condition of light irradiation to suppress the short-term drift.

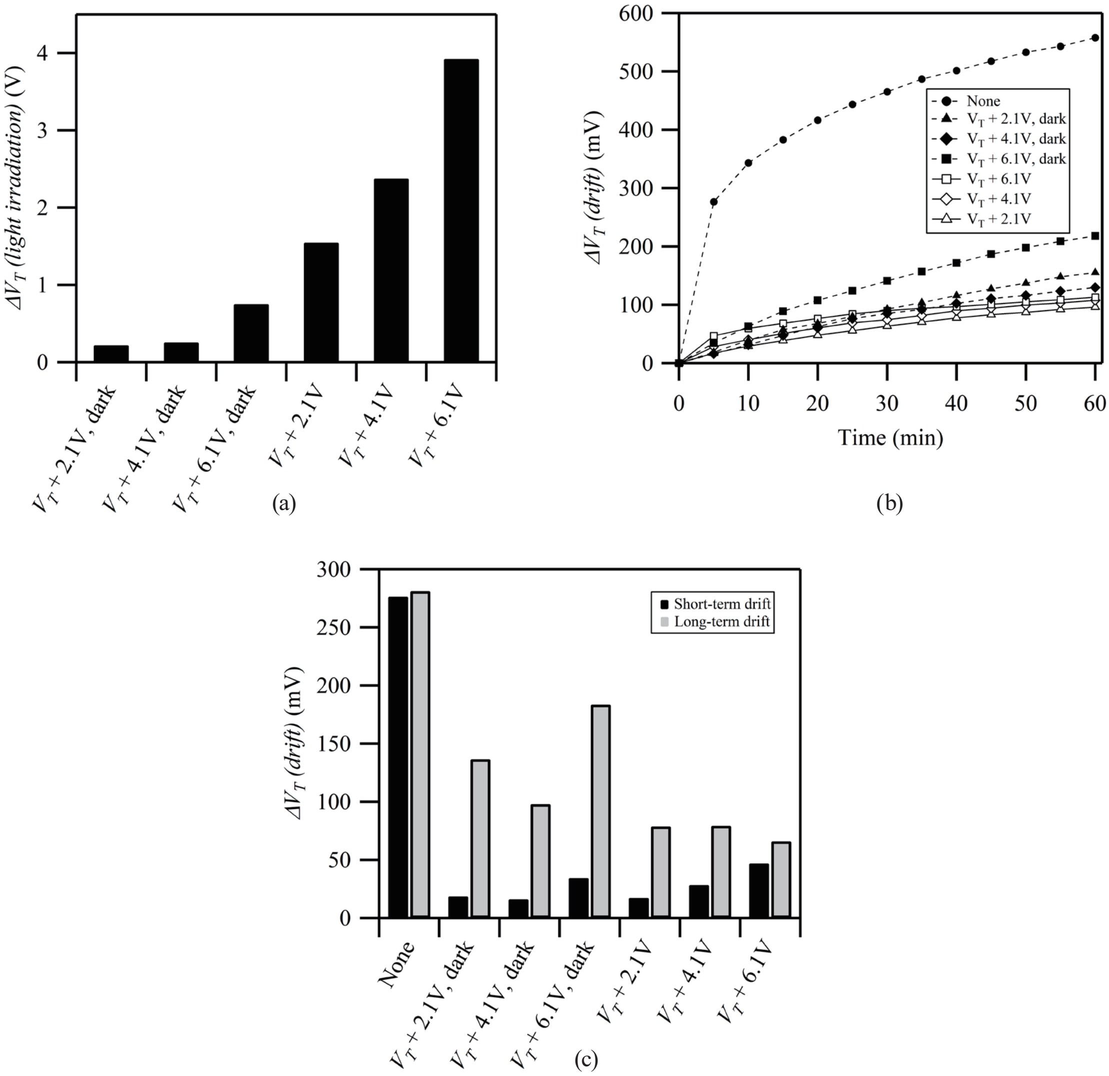


Fig. 4. Effects of UV light irradiation on drift. (a) $\Delta V_T$ induced by bias voltage application with or without light irradiation. (b) Drifts after bias voltage application. (c) Amounts of short-term and long-term drifts.

### 3.4 Effects of duration of light irradiation on drift

As suggested in Fig. 4(c), there may be an optimal light irradiation condition for the suppression of the short-term drift. To investigate the optimal condition, we examined the effect of the duration of light irradiation before the drift measurement. The duration was varied at 5, 30, 60, and 180 s. The bias voltage during light irradiation was set to $V_T$ (2.864 V) + 6.1 V.

Figure 5(a) shows $\Delta V_T$ induced by light irradiation. $\Delta V_T$ induced by light irradiation for 5 min [Fig. 4(a), $V_T$ + 6.1 V] is also shown for comparison. The $\Delta V_T$ values after light irradiation for 5, 30, and 60 s are found to be similar, whereas the longer duration of light irradiation induces a larger $\Delta V_T$. This result indicates that the charge trapping induced by light irradiation includes at least two processes: the fast process that occurs in 5 s, and the slow process that occurs in 3 min. The drifts measured after light irradiation are shown in Fig. 5(b). This result shows that light

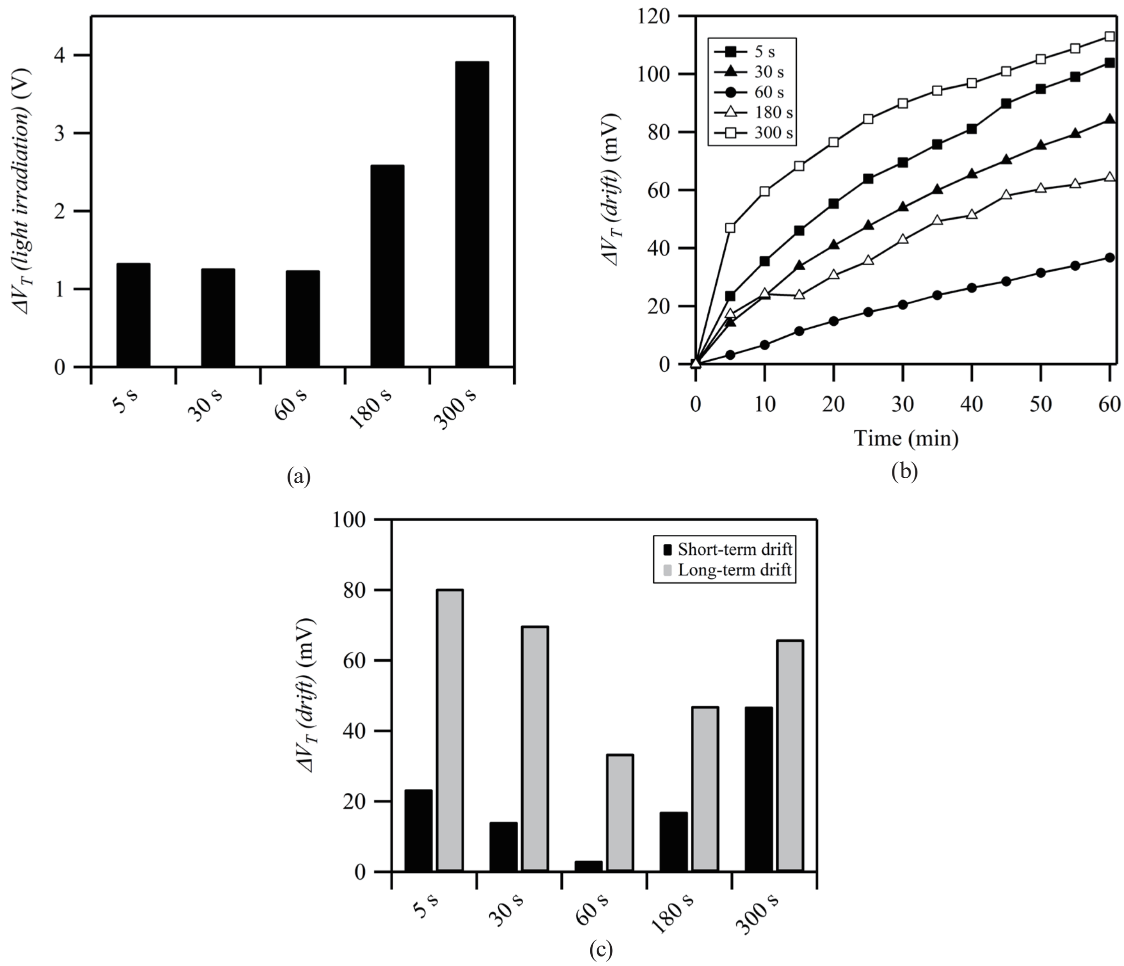


Fig. 5. Effects of duration of UV light irradiation on drift. (a) $\Delta V_T$ induced by UV light irradiation for different durations. (b) Results of drift measurements after UV light irradiation. (c) Amounts of short-term and long-term drift.

irradiation is effective for suppressing the drift even in the case of light irradiation for 5 s [Fig. 5(b), square]. It also shows that light irradiation for 60 s minimizes the subsequent drift. Figure 5(c) presents the short-term (black) and long-term (gray) drifts of each sample. It shows that both the short-term and long-term drifts become smaller with the increase in the duration of light irradiation up to 60 s. In contrast, the amounts of drifts increase in the longer light irradiation durations of 180 and 300 s. These results indicate that light irradiation for 60 s is optimal and that the optimal duration of light irradiation would be shorter than the moment at which the $\Delta V_T$ induced by the slow process becomes evident. The drift after light irradiation for 60 s was 37 mV/h, which is 6.6% relative to the drift under dark conditions (558 mV/h).

## 4. Discussion

As shown in Fig. 3(a), UV light irradiation induced a large positive $\Delta V_T$ and the shoulder of the CV curves in the depletion region disappeared with the increase in the duration of light irradiation. These findings suggest that light irradiation induces the trapping of electrons and fills the trap levels near the interface between $Al_2O_3$ and Si. Since both the short-term and long-term drifts were affected by light irradiation, we consider that the main cause of these drifts is the gradual trapping of electrons under bias voltage application. We speculate that light irradiation suppressed the drift by filling the trap levels and decreasing the efficiency of charge trapping in the subsequent drift measurements. The existence of short-term and long-term drifts, which were affected by light irradiation through different mechanisms, and the existence of fast and slow processes during light irradiation suggest that the drift is caused by multiple charge trapping mechanisms. We consider that these mechanisms depend on the type of trap level (interface and border traps)(18) and the distribution of border traps in $Al_2O_3$.(32) Since light irradiation also affects the charge trapping and detrapping phenomena in the other types of metal oxide layers such as $HfO_2$, $SiO_2$, and $SiN_x$,(24,26–28) it is possible that light irradiation is effective for suppressing the drift of an ISFET, which uses those metal oxides as the sensing layer.

## 5. Conclusions

In this research, we investigated the effects of UV light irradiation on the drift in an ISFET with an $Al_2O_3$ sensing layer by fabricating a wafer sample with the same layer composition and measuring the drift by CV measurements. It was shown that light irradiation induces an increase in $V_T$ and that the drift is suppressed after light irradiation. It was also shown that the shoulder in the CV curve, which is known to be related to the density of interface traps between $Al_2O_3$ and Si,(29) disappeared after light irradiation. These findings indicate that the main cause of the drift is the trapping of electrons by the trap levels in $Al_2O_3$ and that light irradiation reduced the efficiency of trapping by filling the trap levels. The smallest drift after light irradiation was 37 mV/h, which is 6.6% relative to the original drift (558 mV/h). These results suggest that the drift caused by charge trapping may not be negligible in ISFETs and light irradiation can be used as a method to suppress the drift.

## References


1 M. W. Shinwari, M. J. Deen, and D. Landheer: Microelectron. Reliab. **47** (2007) 2025. https://doi.org/10.1016/j.microrel.2006.10.003
2 S. Sinha and T. Pal: Electrochem. Sci. Adv. **2** (2022) e2100147. https://doi.org/10.1002/elsa.202100147
3 P. Bergveld: Sens. Actuators, B **88** (2003) 1. https://doi.org/10.1016/S0925-4005(02)00301-5
4 M. J. Schöning and A. Poghossian: Analyst **127** (2002) 1137. https://doi.org/10.1039/B204444G
5 C. Jimenez-Jorquera, J. Orozco, and A. Baldi: Sensors **10** (2010) 61. https://doi.org/10.3390/s100100061
6 W. Baumann, M. Lehmann, A. Schwinde, R. Ehret, M. Brischwein, and B. Wolf: Sens. Actuators, B **55** (1999) 77. https://doi.org/10.1016/S0925-4005(99)00116-1
7 T. Sakata, S. Nishitani, Y. Yasuoka, S. Himori, K. Homma, T. Masuda, A. M. Akimoto, K. Sawada, and R. Yoshida: Sci. Rep. **12** (2022) 2949. https://doi.org/10.1038/s41598-022-06964-4
8 S. Nakata, T. Arie, S. Akita, and K. Takei: ACS Sens. **2** (2017) 443. https://doi.org/10.1021/acssensors.7b00047
9 H. Horiuchi, M. Agetsuma, J. Ishida, Y. Nakamura, D. L. Cheung, S. Nanasaki, Y. Kimura, T. Iwata, K. Takahashi, K. Sawada, and J. Nabekura: Nat. Commun. **11** (2020) 712. https://doi.org/10.1038/s41467-020-14571-y

10 J. M. Rothberg, W. Hinz, T. M. Rearick, J. Schultz, W. Mileski, M. Davey, J. H. Leamon, K. Johnson, M. J. Milgrew, M. Edwards, J. Hoon, J. F. Simons, D. Marran, J. W. Myers, J. F. Davidson, A. Branting, J. R. Nobile, B. P. Puc, D. Light, T. A. Clark, M. Huber, J. T. Branciforte, I. B. Stoner, S. E. Cawley, M. Lyons, Y. Fu, N. Homer, M. Sedova, X. Miao, B. Reed, J. Sabina, E. Feierstein, M. Schorn, M. Alanjary, E. Dimalanta, D. Dressman, R. Kasinskas, T. Sokolsky, J. A. Fidanza, E. Namsaraev, K. J. McKernan, A. Williams, G. T. Roth, and J. Bustillo: Nature **475** (2011) 348. https://doi.org/10.1038/nature10242
11 T. Matsuo and M. Esashi: Sens. Actuators **1** (1981) 77. https://doi.org/10.1016/0250-6874(81)80006-6
12 L. Bousse, D. Hafeman, and N. Tran: Sens. Actuators, B **1** (1990) 361. https://doi.org/10.1016/0925-4005(90)80231-N
13 Y. Dun, W. Ya-dong, and W. Gui-hua: Sens. Actuators, B **3** (1991) 279. https://doi.org/10.1016/0925-4005(91)80018-F
14 J.-L. Chiang, S.-S. Jan, J.-C. Chou, and Y.-C. Chen: Sens. Actuators, B **76** (2001) 624. https://doi.org/10.1016/S0925-4005(01)00657-8
15 S. Jamasb, S. Collins, and R. L. Smith: Sens. Actuators, B **49** (1998) 146. https://doi.org/10.1016/S0925-4005(98)00040-9
16 J. Zhang, D. Zhao, H. Yang, C. Li, H. Si, and D. Wu: IEEE Sens. J. **19** (2019) 7471. https://doi.org/10.1109/JSEN.2019.2913568
17 S. Kim, D. W. Kwon, S. Kim, R. Lee, T.-H. Kim, H.-S. Mo, D. H. Kim, and B.-G. Park: Curr. Appl. Phys. **18** (2018) S68. https://doi.org/10.1016/j.cap.2017.11.021
18 D. Fleetwood: Microelectron. Reliab. **80** (2018) 266. https://doi.org/10.1016/j.microrel.2017.11.007
19 L. Larcher, A. Padovani, V. della Marca, P. Pavan, and A. Bertacchini: Proc. 2010 Int. Symp. VLSI Technology, System and Application (IEEE, 2010) 52. https://doi.org/10.1109/VTSA.2010.5488951
20 F. Werner and J. Schmidt: Appl. Phys. Lett. **104** (2014) 091604. https://doi.org/10.1063/1.4867652
21 E. Schilirò, R. Lo Nigro, P. Fiorenza, and F. Roccaforte: AIP Adv. **6** (2016) 075021. https://doi.org/10.1063/1.4960213
22 R. Y. Khosa, E. B. Thorsteinsson, M. Winters, N. Rorsman, R. Karhu, J. Hassan, and E. O. Sveinbjörnsson: AIP Adv. **8** (2018) 025304. https://doi.org/10.1063/1.5021411
23 M. M. Rahman, K.-Y. Shin, and T.-W. Kim: Materials **13** (2020) 5809. https://doi.org/10.3390/ma13245809
24 J.-Y. Kwon, J. S. Jung, K. S. Son, K.-H. Lee, J. S. Park, T. S. Kim, J.-S. Park, R. Choi, J. K. Jeong, B. Koo, and S. Y. Lee: Appl. Phys. Lett. **97** (2010) 183503. https://doi.org/10.1063/1.3513400
25 C. Mizue, Y. Hori, M. Miczek, and T. Hashizume: Jpn. J. Appl. Phys. **50** (2011) 021001. https://doi.org/10.1143/JJAP.50.021001
26 K. H. Ji, J.-I. Kim, Y.-G. Mo, J. H. Jeong, S. Yang, C.-S. Hwang, S.-H. K. Park, M.-K. Ryu, S.-Y. Lee, and J. K. Jeong: IEEE Electron Device Lett. **31** (2011) 1404. https://doi.org/10.1109/LED.2010.2073439
27 J. J. Siddiqui, J. D. Phillips, K. Leedy, and B. Bayraktaroglu: J. Mater. Res. **27** (2012) 2199. https://doi.org/10.1557/jmr.2012.173
28 S. Park, E. N. Cho, and I. Yun: J. Soc. Inf. Disp. **21** (2013) 333. https://doi.org/10.1002/jsid.170
29 E. H. Nicollian and J. Brews: MOS (Metal Oxide Semiconductor) Physics and Technology (Willey, New Jersey, 2003), Chap. 2–5.
30 Y.-N. Lee, T. Araki, Y. Kimura, F. Dasai, T. Iwata, K. Takahashi, and K. Sawada: IEEE Trans. Biomed. Circuits Syst. **13** (2019) 352. https://doi.org/10.1109/TBCAS.2019.2895069
31 P. Bergveld: Sens. Actuators **8** (1985) 109. https://doi.org/10.1016/0250-6874(85)87009-8
32 Y. Yuan, L. Wang, B. Yu, B. Shin, J. Ahn, P. C. McIntyre, P. M. Asbeck, M. J. W. Rodwell, and Y. Taur: IEEE Electron Device Lett. **32** (2011) 485. https://doi.org/10.1109/LED.2011.2105241

## About the Authors

**Yasumichi Takase** received his B.A. degree in liberal arts from The University of Tokyo, Tokyo, Japan, in 2015, and his M.A. and Ph.D. degrees in biophysics in 2018 and 2021, respectively, from Nara Institute of Science and Technology, Nara, Japan. Since he joined Kyocera Corporation in 2021, he has been involved in the development of electrochemical sensors for healthcare applications. (yasumichi.takase@gmail.com)

**Takafumi Ishigaki** received his M.S. degree in electrical and electronic engineering from The University of Tokyo, Tokyo, Japan, in 2021. In the same year, he joined Kyocera Corporation, Kyoto, Japan, where he was involved in research on electrochemical sensors for biomedical applications. His current research focuses on developing technologies related to image analysis for medical devices, encompassing both electronic components and algorithmic design. (takafumi.ishigaki.hs@kyocera.jp)

**Shinnosuke Nakamura** received his M.S. degree in applied chemistry from The University of Tokyo, Tokyo, Japan, in 2012. Since joining Kyocera Corporation in 2012, he has been involved in the development of biosensors based on surface acoustic wave devices. He is currently working on a new business development using sensors. (shinnosuke.nakamura.sd@kyocera.jp)

**Hideaki Asao** received his M.S. degree in applied physics from Hokkaido University, Hokkaido, Japan, in 2007. Since joining Kyocera Corporation in 2007, he has been involved in the development of thin-film processes and thin-film devices, particularly solar cells and piezoelectric devices. He currently serves as the manager of an electronic device development section in the R&D division. (hideaki.asao.ke@kyocera.jp)

**Tomoko Horio** is a research assistant at Toyohashi University of Technology. She received her B.S. degree in agriculture from Gifu University in 2001. She is working on the characterization of bioimaging devices based on electrochemical sensors. (horio-t@int.ee.tut.ac.jp)

**Takeshi Hizawa** received his B.A. and M.S. degrees in electrical and electronic engineering and his Ph.D. degree in electronic and information engineering, all from Toyohashi University of Technology, Aichi, Japan, in 2002, 2004, and 2007, respectively. From 2007 to 2013, he worked at Toshiba Corp. He was engaged in the development of semiconductor process technology. In 2013, he joined Toyohashi University of Technology, where he is now serving as a technical support staff member for semiconductor devices and process technology. (hizawa@ts.tut.ac.jp)

**Yasuyuki Kimura** received his B.E. degree from Tsukuba University in 1982. He joined SANYO Electric Co., Ltd. in 1982 and was in charge of developing Mixed-Signal LSIs. Since 2014, he has been a research fellow at the Department of Electrical and Electronic Information Engineering of Toyohashi University of Technology. (kimura.yasuyuki.db@tut.jp)

**Kazuaki Sawada** was born in Kumamoto, Japan in 1963. He received his B.A. and M.S. degrees in electrical and electronic engineering in 1986 and 1988, respectively, and his Ph.D. degree in system and information engineering in 1991, all from Toyohashi University of Technology (TUT), Aichi, Japan. From 1991 to 1998, he was a research associate at the Research Institute of Electronics, Shizuoka University, Shizuoka, Japan. In 1998, he joined the Department of Electrical and Electronic Engineering, TUT, where he is now serving as a full professor. Professor Sawada is a director of the Institute for Research on Next-Generation Semiconductor and Sensing Science (IRES2), TUT. He was a guest professor at the Technical University of

Munich in 2005. His current research interests focus on the development of nonlabel bio-image sensing devices and multimodal sensors for ion image sensing devices. Professor Sawada was a recipient of the Prizes for Science and Technology, the Commendation for Science and Technology by the Minister of Education, Culture, Sports, Science and Technology, Japan 2012. (kazuaki.sawada@tut.jp)

**Astuomi Fukuura** received his M.S. degree in physics from Kwansei Gakuin University, Nishinomiya, Japan, in 1990, and his M.Eng. degree in electrical engineering from McMaster University, Hamilton, ON, Canada, in 1999. Since joining Kyocera Corporation in 1990, he has been engaged in numerical techniques for the analysis and design of microwave/optical components as well as in the R&D of novel sensor devices for healthcare applications. His current interest includes software sensing technologies and the data-driven modeling of complex systems.